VIBRATION MEASUREMENT OF AN EDGE CRACKED COMPOSITE PLATE BY AMPLITUDE FLUCTUATION ESPI METHOD

WEI-CHUNG WANG and CHI-HUNG HWANG
Department of Power Mechanical Engineering, National Tsing Hua University
Hsinchu, Taiwan 30043, Republic of China

ABSTRACT

In this paper, the amplitude fluctuation(AF) electronic speckle pattern interferometry (ESPI) method was adopted to investigate the vibration characteristics of a composite plate containing a single edge crack. The change of the modal shapes was discussed. In addition, the stress intensity factors(SIFs) induced by vibration were evaluated.

KEYWORDS

Composite plate, Vibration, ESPI, Edge crack.

INTRODUCTION

When composite structures are in service, occasionally, cracks are introduced due to accidental impact or environmental contamination. Therefore, dynamic properties of composite structures may be changed. Vibration modes different from those generated by defect-free composite structures and stress intensity factors(SIFs) induced by vibration are produced. Structures may then be failed because of the large displacement introduced by additional resonance or crack prorogation.

To evaluate dynamic characteristics of a cracked composite plate, in this paper, the electronic speckle pattern interferometry(ESPI) method was used. The ESPI method is a real-time, high measurement sensitivity(5~100μm)(Jones and Wykes, 1983) whole-field and non-contact experimental method. For vibration measurement, Butters and Leendertz(1971) first employed the ESPI method on a disc. From then on, the development of the ESPI method has focused on increasing the measurement sensitivity. Lϕkberg and Hϕgmoen(1976) combined the time-averaged ESPI method with the phase modulation technique to obtain the contours of constant phase. Hϕgmoen and Lϕkberg (1977) proposed that the sensitivity of the vibration measurement can be increased by driving a modulating mirror at a frequency which is slightly different from the vibration of the object. Besides, Santoyo, *et al,* (1991) applied the ESPI method for in-plane vibration measurement. Shellaber and Tyrer (1991) set up a three dimensional ESPI optical arrangement to measure the vibration of a turbocharger blade, a thick annular cylinder and a center-pinned free square plate to prove that the orthogonal displacement components can be measured individually.

As for fracture problems, a crack subjected to an in-plane or out-of-plane periodic stress loading in an infinite or semi-infinite domain was investigated(Patron and Boriskovsky, 1989).

As for the finite domain problems, Boriskovsky *et al.*(1982) used the finite element method to determine the SIFs of a finite cracked body subjected to a harmonic loading, the SIFs at any vibration frequencies were assumed as the superposition of the modal SIFs corresponding to the normalized free vibration modes with associated weight coefficients. A discussion on the vibration of sectorial plates was reported by Leissa *et al.*(1993a), different from the traditional studies about the sectorial plates, stress singularities have been put into consideration. Furthermore, Leissa *et al.*(1993b) considered the vibration of circular plates which include a v-notch or sharp radial crack. By applying the Ritz method, the total displacements were assumed to be composed of two parts: the functions of the displacements are the polynomial function and the corner function, thus the exact solution for free vibrations of sectorial plates with simply supported radial edges was also established by Huang et al.(1994). The importance of the stress singularities was also emphasized. However, the above studies are all focused on the vibration behaviors not on the stress signularity.

In this paper, the amplitude fluctuation(AF) ESPI method - a new ESPI measurement method which was proposed by the authors(Wang, et al. 1995) was adopted. The measurement sensitivity of the AF ESPI method is increased without additional optical devices. By using this method, vibration characteristics of an edge cracked composite plate were evaluated and discussed.

THEORY

The Amplitude Fluctuation ESPI Method(Wang et al., 1995)

The AF ESPI method for vibration measurement is based on the video signal subtraction method which has been widely used to evaluate the steady state displacement field(Jones and Wykes, 1983). However, the reference image in the AF ESPI method is no longer being taken from the stress-free state but a vibrating state instead. The out-of-plane ESPI optical setup, as shown in left side of Fig. 1, is used in this paper. Note that even for a periodic vibrating motion, the vibration amplitude would be slightly changed during each cycle because of the environmental or electronic noises of the vibration system. Therefore, the amplitude can be assumed to change from A into $A+\Delta A$ for each cycle, where ΔA is a rather small disturbance. By the real-time operation function of image-processing system, the brightness displays on the monitor can be expressed as

$$B_{IM} = \frac{4N\alpha\beta\pi\sqrt{I_o I_r}}{\omega}[J_1^2(k)\cos^2\varphi]^{1/2} \tag{1}$$

where N = fringe order; α = the slope of CCD camera's sensitivity curve; ω = vibration frequency; φ = the random phase due to the surface roughness; $k = 2A\pi(1+\cos\theta)/\lambda$; I_o = the object light beam; I_r = the reference light beam; λ = wave length of the light source; θ = the illumination angle of the object light and β = the conversion factor of look up table of the image processing system. Based on eq.(1), the vibration amplitude of the specimen can be obtained by a set of $k=\zeta_i$ which can null eq. (1), then the related amplitude is

$$A = \lambda\zeta_i / 2\pi(1+\cos\theta) \tag{2}$$

Evaluation of Stress Intensity Factors

Based on the research of Leissa *et al.*(1993a), the displacement of an edge cracked composite plate, w_t, can be decomposed into two parts: the principal displacement, w_p, and the singular displacement, w_s, i.e.,

$$w_t = w_p + w_s \tag{3}$$

The motion equation of the orthotropic composite plates can be expressed as(Vinson and Sierakowski, 1986)

$$D_{11}\frac{\partial^4 w_t}{\partial x^4} + 2(D_{12}+D_{66})\frac{\partial^4 w_t}{\partial x^2\partial y^2} + D_{22}\frac{\partial^4 w_t}{\partial y^4} = \rho\frac{\partial^2 w_t}{\partial t^2} + q(x,y,t) \tag{4}$$

where xy is the structural coordinate; ρ is the mass density of the composite plate; q(x,y,t) is the distributed load; $D_{ij} = 1/3\sum_{k=1}^{16}(\overline{Q}_{ij})_k[h_k^3 - h_{k-1}^3]$ with i, j =1, 2, 6; h_k is the thickness of the k-th lamina; and $\overline{Q}_{ij}$ is the component of $[\overline{Q}]$ which can be related with the stiffness matrix [Q] of the laminae in fiber direction as $[\overline{Q}] = [T]^{-1}[Q][T]$, where [T] is the coordinate transfer function between structural coordinate and the fiber coordinate of laminae.

Substituting eq. (3) into eq.(4) and assuming that w_p and w_s possess the following characteristics

$$w_p(x,0^+) - w_p(x,0^-) = 0;\ w_s(x,0^+) - w_s(x,0^-) = \delta(x),\ -a \le x \le 0 \tag{5}$$

where $\delta(x)$ is the crack opening function along crack and a is the crack length.

Besides, since w_s is caused by the singularity of the crack, the singularity can be of the form

$$w_s(x,y) = w_s(r,\theta) = f(\sqrt{r},\theta) \tag{6}$$

where $r\theta$ is polar coordinate commonly used in fracture mechanics.

With eq. (6), w_s will be at least an order smaller than w_p. Eq. (4) can be decomposed into two equations, i.e.,

$$D_{11}\frac{\partial^4 w_p}{\partial x^4} + 2(D_{12}+D_{66})\frac{\partial^4 w_p}{\partial x^2\partial y^2} + D_{22}\frac{\partial^4 w_p}{\partial y^4} = \rho\frac{\partial^2 w_p}{\partial t^2} + q(x,y,t) \tag{7-a}$$

$$D_{11}\frac{\partial^4 w_s}{\partial x^4} + 2(D_{12}+D_{66})\frac{\partial^4 w_s}{\partial x^2\partial y^2} + D_{22}\frac{\partial^4 w_s}{\partial y^4} = 0 \tag{7-b}$$

The problem of an edge cracked plate can be decomposed into two problems, one is the vibration of cracked plate with an assumed displacement across the crack, and one is with non-uniform shear stress distribution along the crack surface. Consequently, the SIFs of a edge cracked plate can be evaluated if the SIFs of a steady-state crack subjected to a distributed loading can be evaluated.

In this paper, the SIFs of an edge cracked composite plate were evaluated by the displacement field. Only the out-of-plane displacement, w, can be measured by the ESPI in this paper, i.e., mode-III SIFs were investigated. In isotropic cases, mode-III displacement problems can be expressed as(Hellan, 1984)

$$w = (K_{III}/G)(\sqrt{2r/\pi})\sin(\theta/2) \tag{8}$$

where G is the shear modulus. From eq. (8), the displacement difference between crack surfaces can be expressed as

$$\Delta w = w|_{\theta=\pi} - w|_{\theta=-\pi} = (2\sqrt{\pi}K_{III} / G)\sqrt{r} \quad (9)$$

Based on eq. (9), the SIFs can be evaluated by computing the slope of Δw-$\sqrt{r}$ plot.

SPECIMEN AND EXPERIMENTAL SETUP

Test Specimen

As depicted in Fig. 2, a specimen with a crack of length 40 mm on the edge of a composite plate of stacking sequence $[0]_{16}$ was used for study. In this experiment, the composite plate was produced from the 250 mm x 250 mm unidirectional CFRP prepreg and then cured by the vacuum bag method. The cured CFRP plate was cut into several 200 mm x 90 mm sheets by using a diamond wheel. To produce the crack, a screw slotting cutter of 0.35 mm thick was used. Dash line in Fig. 2 is used to indicate regions A and B for later discussion.

Experimental Setup

The experimental setup, as shown in Fig. 1, used in this experiment can be classified into two systems. They are the vibration and ESPI systems. In this paper, the vibration system was used to determine the natural frequencies and associated modes. Besides, the vibration system was also used to offer the sinusoidal exciting force for ESPI vibration measurement. Devices and components which were used to construct the vibration system are shaker(LDS Co., U.K.), an accelerometer(PCB Co., U.S.A.), a function generator(Levell Electronics Co., U.K.), and a PC based spectrum analyzer(ProWave Co., R.O.C.) which was used to evaluate the frequency response functions(FRFs) of every measurement points and also used to monitor the exciting force.

The ESPI system consist of two parts: The ESPI out-of-plane optical setup and the real-time operation image processing system with associated software. As for the ESPI out-of-plane optical setup, a 35 mW He-Ne laser of wavelength 632.8 nm was used as light source. A ground glass was added into the reference beam arrangement so that the optical collinearity can be more easily achieved. In this paper, AFG(Imaging Technology Co., U.S.A) image processing board was adopted because of its real-time processing capability. To perform the real-time image operation, computer programs were developed. In this paper, the time-averaged technique was applied with the AF ESPI method. Whenever the time-averaged technique was used to study the vibration problems, the shutter opening period must be the same or the multiple of the vibration period to avoid possible mistakes(Wang *et al.*, 1995).

A CCD camera is used to conjoint the out-of-plane ESPI optical setup with the image processing system. Since the time difference between CCD shutter opening period and vibration period need to be adjusted , an integration CCD(Plunix Co. of U.S.A.) camera with cooling function was used.

In this paper, the modal testing technique was first applied to find modal frequencies for convenience. Whenever modal frequencies were found, the output frequencies of the function generator were set to the same ones as the modal frequencies. By using the AF ESPI method, the vibration amplitude can be measured.

RESULTS AND DISCUSSIONS

Physical Interpretation of Modes of an Edge Cracked Composite Plate

Fringe patterns of the first six modes of a $[0]_{16}$ edge cracked composite plate are shown in Fig. 3. Fringes of the first mode shown in Fig. 3(a) on region B are parallel to each other. However, fringes in region A begin to rotate. Since the introduction of the crack generates new free surfaces, those new free surfaces cannot constrain the displacement of region A. Consequently, the out-of-plane bending rigidity would be reduced. The reduction of the bending rigidity would make the composite plate to perform easier an out-of-plane rotation and hence large deformation demonstrated at region A. As for the second mode(Fig. 3(b)), all fringes in region A are almost parallel to the fiber direction. Note that the $[0]_{16}$ composite plate only has fiber in the longitudinal direction, i.e., Y direction. Basically, the type of deformation of the second mode is a twist mode. In other words, an equivalent twist moment M_{yx} is applied on the plate. Since the free surface introduced by the crack has no capability to resist the twist bending, larger displacement has occurred in region A. Moreover, the composite plate has rather weak bending rigidity perpendicular to the fiber direction because there is resin only, therefore, displacement along the fiber was kept constant. Fringe patterns of the third and fourth modes are shown in Figs. 3(c) and 3(d), respectively. Similar to the first mode, displacement in region A is increased because of the new free surfaces introduced by the crack and hence the reduction of the bending moment rigidity. For higher frequency vibration modes as shown in Figs. 3(e) and 3(f), region B has significantly larger displacement than region A. Since the shaker was used to provide the exciting load, as the modal frequencies increase the stroke of the shaker decreases. Owing to the limitation of the stroke of the shaker, the displacement of the plate will be smaller everywhere. However, mass will become significant when a structure experiences higher frequency vibration. Observing the fringe patterns in Figs. 3(e) and 3(f), all fringes are almost parallel to each other in region B. Those fringe patterns were clearly caused by the mass of region B. Due to the newly introduced free surfaces, region B rotates freely and gains a larger displacement. Note that the mass effect of region B is also acting on regions outside the region B. However, complex modes always introduce more nodal lines, and the existence of nodal lines can be seen as solid boundaries with zero-displacement and thus larger deformation is prevented to occur in the structure.

According to those fringes of the first six modes shown in Fig. 3, the displacement around the crack can be classified into three types. They are the in-phase displacement, out-of-phase displacement and the complex displacement. For the in-phase displacement cases, i.e., the first, third and fourth modes, bending displacement in the longitudinal direction occurs in the edge cracked plate. For the out-of-phase displacement cases, such as the second and sixth modes, the twist displacement with respect to the longitudinal axis occurs in the edge cracked plate. For the complex deformation case, i.e., the fifth mode, a nodal line perpendicular to the crack surface occurs, and local effect about the crack shows up.

Stress Intensity Factors

Assuming that SIF of an orthotropic material has the same form of eq. (9), i.e., $K^*_{III} = \Delta w / \sqrt{r}$, where $K^*_{III} = K_{III}C(D_{ij})$, C is a function of D_{ij}. Plot of Δw versus $\sqrt{r}$ for all the first six modes is shown in Fig. 4. It is clear that the Δw correlates linearly with $\sqrt{r}$ when $\sqrt{r} > 1$. Therefore, K^*_{III} for the first six modes can be determined when $\sqrt{r} > 1$ and compared to each other. It is clear that the fifth mode has the highest singularity while the first mode has the lowest singularity. Since mode-III is a tear mode, the larger the out-of-

plane difference introduced by the free surfaces of the crack, the stronger singularity of K^*_{III}. Although the fifth mode has been classified as the complex displacement type because of there is a nodal line, N-N, exist in region A and perpendicular to the crack. The fringe orders on the right side of the nodal line are of the different phase of the fringes in region B, i.e., whenever region A on the right side of the nodal line move in the positive z direction, region B would move in the negative z direction. Since the fifth mode will perform out-of-phase displacement on the right side of the nodal line, largest out-of-phase displacement difference is then reached. The other case is the second mode which also perform out-of-phase displacement in region A, therefore the SIF of the second mode is just less than the SIF of the fifth mode.

It is worth of noting that, the fringe patterns were not obtained by the same exciting force. However, the difference of maximum displacements of all six modes are small. When a structure subjected to a resonant loading, two failure criteria may be adopted to investigate the reliability of the structure. They are the displacement criterion and the stress criterion. From the obtained fringe patterns, it can be clearly observed that the maximum displacement of the fifth mode is about one fringe order less than the first four modes. Therefore, the fifth mode may be accepted by the displacement criterion, however, with higher SIF of this mode, the plate may be failed due to the existence of the crack.

CONCLUSIONS

In this paper, the AF ESPI method was first used to obtain vibration fringe patterns of an edge cracked composite plate. In-phase, out-of-phase and complex displacements all can possibly be produced. Free surfaces caused by the crack play an important role in the vibration configuration. For higher frequency vibration, mass of the plate becomes important. The SIFs of the first six modes were determined by the modal shapes and the displacement differences between free surfaces of the crack. From the obtained experimental results, larger value of SIFs is not necessarily corresponding to larger displacement. In the traditional vibration design concept, displacement dominant failure has always been adopted for a defect-free structure. However, according to the results of this paper, if there is a crack exists in the structure, the stress-related fracture criterion must be considered, especially for higher frequency vibration.

ACKNOWLEDGMENTS

This research was supported in part by the National Science Council(Grant Nos. NSC 82-0401-E007-299, NSC 82-0618-E007-323, NSC 83-0401-E007-007 and NSC 84-2212-E007-062) of the Republic of China.

REFERENCES

Boriskovsky, V. G., E. M. Dashevsky , and L. D. Denisov, (1982). On the Dynamic Stress Intensity Factors in Finite Cracked Bodies Under Harmonic Loading. *Engineering Fracture Mechanics*, **16**, 495-465.

Butters, J. N. and J. A. Leendertz,(1971). Holographic and Video Techniques Applied to Engineering Measurement. *J. Measurement and Control*, **4**, 349-354.

Jones, R. and C. Wykes, (1983). *Holographic and Speckle Interferometry*, Cambridge University Press, Cambridge, Massachusetts.

Hellan, K.(1984). *Introduction to Fracture Mechanics*. McGraw-Hill, New York.

Hϕgmoen, K. and O.J. Lϕkberg, (1977). Objection and Measurement of Small Vibration Using Electronic Speckle Pattern Interferometry. *Applied Optics*, **16**, 1869-1875.

Huang, C. S., O. G. McGee and A. W. Leissa, (1994). Exact Analysis Solutions For Free Vibrations of Thick Sectorial Plates with Simply Supported Radial Edges. *Int. J. Solids Structures*, **31**, 1609-1631.

Leissa, A. W., O. G. McGee and C. S. Huang, (1993a). Vibrations of Sectorial Plates Having Corner Stress Singularities. *Journal of Applied Mechanics*, **60**, 134-140.

Leissa, A. W., O. G. McGee and C. S. Huang, (1993b). Vibrations of Circular Plates Having V-notches or Sharp Radial Cracks. *Journal of Sound and Vibration*, **162**, 227-239.

Lϕkberg, O.J. and K. Hϕgmoen, (1976). Vibration Phase Mapping Using Electronic Speckle Pattern Interferometry. *Applied Optics*, **15**, 2701-2704.

Parton, V. Z. and V. G. Boriskovsky, (1989). *Dynamic Fracture Mechanics Volume 1: Stationary Cracks.*(Hetnarski, R. B. ed.), Hemisphere Publishing Co. New York.

Wang, W. C., C. H. Hwang, and S. Y. Lin, (1995). On Vibration of Composite Plates by Time-Averaged ESPI Technique. *Proceedings of the International Symposium on Advanced Technology in Experimental Mechanics*, 329-334, Tokyo, Japan.

Shellabear, M. C. and J. R. Tyrer, (1991). Application of ESPI to three-dimensional Vibration Measurements. *Optics and Lasers in Engineering*, **15**, 43-56.

Santoyo, F. M., Shellabear, J. R. and J. R. Tyrer, (1991) Whole Field In-plane Vibration Analysis Using Pulsed Phase-Stepped ESPI. *Applied Optics*, **30**, 717-721.

Vinson, J. R. and R. L. Sierakowski, (1986). *The Behavior of Structures Composed of Composite Materials*. Martinus Nijhoff Publishers, Netherlands.

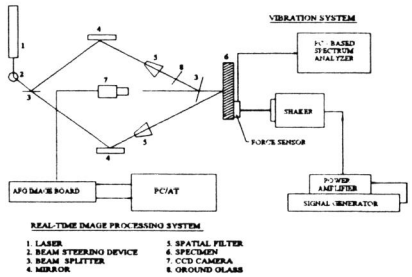

Fig. 1 Schematic of the assembled experimental setup

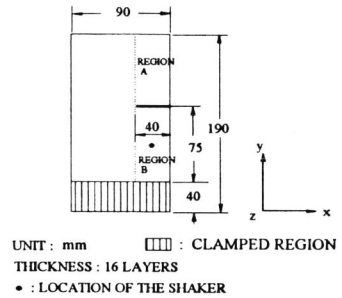

Fig. 2 Test specimen

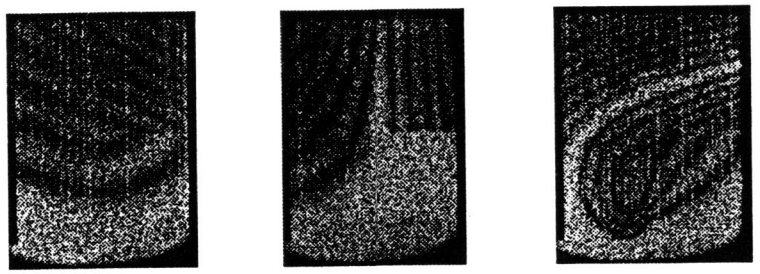

(a) first mode (b) second mode (c) third mode

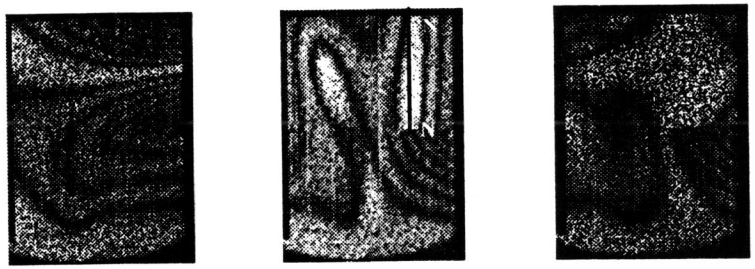

(d) fourth mode (e) fifth mode (f) sixth mode

Fig. 3 Fringe patterns of the first six modes of $[0]_{16}$ composite plate obtained by the AF ESPI method

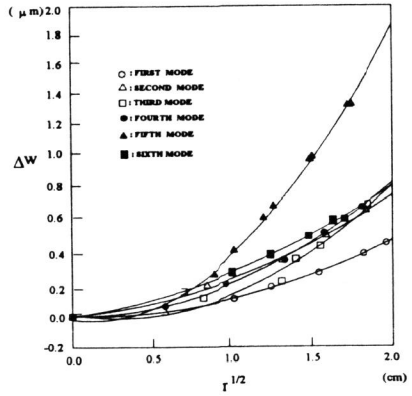

Fig. 4 The Δw-$\sqrt{r}$ plot of first six modes